

Tropical cyclogenesis and mid-level vorticity

David J. Raymond¹, Saška Gjorgjievska¹, Sharon Sessions¹ and Željka Fuchs²

¹New Mexico Tech, Socorro, NM, USA

²University of Split, Split, Croatia

(Manuscript received January 2014; revised March 2014)

This paper reviews and summarises our work on the thermodynamics and vorticity dynamics of tropical cyclogenesis with special emphasis on the use of observations from two recent field programs, T-PARC/TCS08 (THORPEX Asian Regional Campaign/Tropical Cyclone Structure experiment) and PREDICT (PRE-Depression Investigation of Cloud systems in the Tropics). Dropsondes deployed from high altitude plus airborne Doppler radar data (in T-PARC/TCS08) allowed examination of candidates for tropical cyclogenesis in unprecedented detail. The subtle interplay of dynamics and thermodynamics and, in particular, the role of the mid-level vortex in enabling spin up of a surface cyclone are elucidated. The interplay between this process and other investigators' ideas about cyclogenesis is examined also. Finally, those areas of cyclogenesis needing further work are enumerated.

Introduction

Bruce Morton delighted in explaining the finer points of the dynamics of vorticity. The senior author of this paper certainly benefited from his masterful expositions on the subject. Tropical cyclones are creatures of vorticity and convection, and we are honoured to be asked to expound on the subtle interactions between atmospheric vorticity and deep convection in their formation and growth in this volume.

There is general agreement that tropical cyclones develop over warm oceans (sea surface temperature $\geq 26^\circ\text{C}$), away from the equator, and in environments of low vertical shear (e.g. Gray 1968). Beyond that, they almost never develop *ab initio*, but require a pre-existing disturbance to get them started.

It was recognised early on that tropical easterly waves provide a favourable environment for tropical cyclone development (Dunn 1940, Riehl 1948, Palmer 1952, etc.), though only a small fraction of such waves intensify. Other types of disturbances, particularly those related to the monsoon trough in the west Pacific (Ritchie and Holland 1999) as well as mixed Rossby-gravity waves in this region (Dickinson and Molinari 2002) can foster cyclogenesis also. Cyclogenesis in the subtropics is sometimes caused by mid-latitude disturbances as well, e.g. tropical storm *Diana* (1984) in the Atlantic (Bosart and Bartlo 1991) and

storms related to the tropical upper tropospheric trough in the northwest Pacific (Sadler 1976, 1978).

Barotropic instability may play a role in the development of easterly waves and their evolution into tropical cyclones. Molinari et al. (1997), Maloney and Hartmann (2001) and Hartmann and Maloney (2001) found that easterly waves passing through a region of barotropic instability in the east Pacific and southwest Caribbean tended to intensify. Similar regions of instability related to a reversal in the meridional potential vorticity gradient were found by Dickinson and Molinari (2000) over west Africa and northern Australia. A related process is the breakdown of the intertropical convergence zone (ITCZ) by barotropic instability (Ferreira and Schubert 1997, Wang and Magnusdottir 2005, 2006).

In many cases, cyclogenesis appears to result from the interaction of a low-level disturbance, such as a tropical wave, with an upper-level disturbance (Riehl 1948, Sadler 1976, 1978, Molinari et al. 1995). This interaction has been correlated empirically with the existence of upper-level mass divergence (Riehl 1948) and the convergence of eddy fluxes of angular momentum (Pfeffer 1956, 1958, Challa and Pfeffer 1980, Pfeffer and Challa 1981, Challa et al. 1998). Montgomery and Farrell (1993) proposed a mechanism for tropical cyclogenesis resulting from upper-level balanced dynamics. In their model, quasi-geostrophic lifting is greatly amplified in regions that exhibit effective moist-neutral stability due to pre-existing convection. This lifting is sufficient to spin up a tropical cyclone in their model.

A series of field programmes in the early 1990s led to new insights into the process of tropical cyclogenesis.

Corresponding author address: David J. Raymond, Physics Department and Geophysical Research Center, New Mexico, 87801 USA. Email: raymond@kestrel.nmt.edu.

A number of such programmes in the western Pacific during this period documented the role of mid-level vortices from mesoscale convective systems in tropical cyclone formation (Ritchie and Holland 1993, 1997, Simpson et al. 1997, Harr et al. 1996a, 1996b). If these vortices were strong enough or if they merged, the circulation would somehow develop downward to the surface, resulting in the formation of a tropical cyclone. Bister and Emanuel (1997) and Raymond et al. (1998) observed that tropical cyclogenesis in the eastern Pacific was preceded by the formation of a mid-level vortex as well. The models of Bister and Emanuel (1997), Rogers and Fritsch (2001), and Nolan (2007) illustrate this type of development.

Nolan's (2007) paper is particularly interesting in that all numerical simulations of tropical cyclogenesis either developed a mid-level vortex or intensified an existing one before producing the low-level vortex related to cyclogenesis. This occurred even when the simulation was initiated by a low-level vortex. However, in all cases, the column had to be strongly moistened before cyclogenesis occurred. Initiating the simulation with high humidity sped up the process of cyclogenesis. Nolan did point out that there are occasional cases that apparently develop entirely from the bottom up. In particular, numerical simulations suggest that Humberto (2001) formed in the subtropics in this manner as a result of complex interactions with other systems (Davis and Bosart 2006). The frequency of this formation mechanism is not known.

The result of Rogers and Fritsch (2001) is interesting also, in that it shows that a long-lived mid-level vortex over land can lead to the development of a surface circulation as well.

The development of hurricane *Diana* (1984) off the Florida coast was accompanied and perhaps aided by the formation of convective-scale vortices that stood out on satellite imagery (Bosart and Bartlo 1991; Davis and Bosart 2001, 2002). This led to the 'vortical hot tower' hypothesis of Hendricks et al. (2004) and Montgomery (2006), in which such vortices are shown to merge into a larger vortex that evolves into the tropical cyclone. Vortical hot towers are strong convective systems whose behaviour is assumed to be affected significantly by their development in a vorticity-rich environment. A close look at a possible vortical hot tower in developing Atlantic hurricane *Ophelia* (2005) was obtained during RAINEX (Hurricane *Rainband* and Intensity Change Experiment; Houze et al. 2006).

Dunkerton et al. (2009) proposed that tropical cyclogenesis in tropical waves occurs within a 'pouch' surrounding a 'sweet spot' defined by the intersection of the wave axis with a critical latitude at which the phase speed of the wave equals the westward flow speed in the lower troposphere. Given that such waves typically occur in the presence of a low-level easterly jet, there are typically two such latitudes: the poleward one exhibiting anti-cyclonic relative vorticity in the mean flow, and the equatorward one with cyclonic vorticity. The latter is the favoured latitude, as the ambient cyclonic vorticity in conjunction with the vorticity of the

wave itself provide a high-vorticity environment favourable for cyclogenesis. The flow around this sweet spot takes the form of a closed circulation or pouch that acts to suppress the inflow of dry environmental air, thus allowing the convection to further moisturise the environment, leading to tropical cyclogenesis. The combination of high humidity and strong vorticity are thought to lead to the development of vortical hot towers in the pouch as described above. Though Dunkerton et al. (2009) recognise the frequent existence or development of a mid-level vortex during tropical cyclogenesis, they consider this vortex to be incidental to the spinup of a vortex at low levels.

The numerical simulations of Bister and Emanuel (1997), Rogers and Fritsch (2001), and Nolan (2007) suggest that the mid-level vortex is actually a key player in the spin up of a tropical cyclone. Recent numerical simulations of convection by Raymond and Sessions (2007) support this idea. The concept of gross moist stability and its relationship to convective vertical mass flux profiles (Raymond et al. 2009) as well as the balanced thermodynamic response of the environment to mid-level vorticity (Raymond 2012) provide theoretical support for the role of the mid-level vortex. In particular, the modified virtual temperature profile occurring in the presence of such a vortex appears to be favourable to the development of convective mass flux profiles consistent with strong low-level convergence of mass and vorticity, thus favouring the spin up of a low-level cyclone.

The last decade has thus produced a proliferation of ideas about tropical cyclogenesis. Given this background, two recent field programmes have the potential to produce a leap in our understanding of tropical cyclogenesis as new hypotheses are tested against extensive new observations. In 2008, the THORPEX Asian Regional Campaign/Tropical Cyclone Structure experiment (T-PARC/TCS08) studied tropical storm formation near Guam in the western Pacific, while in 2010 the PRE-Depression Investigation of Cloud systems in the Tropics (PREDICT) did the same for Atlantic and Caribbean systems from a base in St. Croix. Both projects deployed dense networks of dropsondes from high altitude (10 km for T-PARC/TCS08 and 13 km for PREDICT) into candidate disturbances for tropical cyclone formation. In addition, T-PARC/TCS08 collected high-quality airborne radar data using ELDORA (ELectra DOppler RADar). Analyses of these data are providing a picture of tropical cyclogenesis in unprecedented detail.

The purpose of this paper is to present systematically the case for the importance of the mid-level vortex to tropical cyclogenesis. The theoretical ground needed for an understanding of this case is first covered. Next, we apply these concepts to the observations obtained in TPARC/TCS08 and PREDICT. Finally, we summarise and discuss these results. We hasten to point out that our analysis does not contradict the idea of a sweet spot within a pouch in tropical cyclogenesis, but complements it. Only with the protection provided by the pouch can the thermodynamic processes envisioned here act to promote genesis. However it does

require that the concept of the pouch be extended in depth to include important processes in the middle troposphere. Our findings indicate that the special form of convection leading to cyclogenesis in the pouch cannot be understood without considering the role of the mid-level vortex.

Vorticity dynamics

The dynamics of vorticity was Bruce Morton's love. He would have appreciated certain subtle aspects of this subject discussed here.

We begin with the horizontal momentum equation written in the form expressed by Raymond and López (2011),

$$\frac{\partial \mathbf{v}_h}{\partial t} + \nabla_h(v^2/2) + \mathbf{k} \times \mathbf{Z} + \nabla_h(\theta_0 \Pi) = 0, \quad (1)$$

where $\mathbf{v}=(v_r, v_\theta)$ is the velocity field, ∇_h is the horizontal gradient operator, \mathbf{k} is the vertical unit vector, θ is the virtual potential temperature, $\Pi = C_p(p/p_R)^\kappa$ is the Exner function, C_p is the specific heat of air at constant pressure, p is the pressure, p_R is a constant reference pressure (typically 1000 hPa), and $\kappa = R/C_p$ where R is the gas constant for air. A subscripted h indicates the horizontal component of a vector.

In (1) we have divided the potential temperature into barotropic and baroclinic parts, $\theta = \theta_0(z) + \theta'$ and note that $\theta_0 \nabla_h \Pi = \nabla_h(\theta_0 \Pi)$. The baroclinic part is absorbed into \mathbf{Z} , which is the horizontal flux of the vertical component of absolute vorticity ζ_z :

$$\mathbf{Z} = \mathbf{v}_h \zeta_z - \zeta_h v_z + \mathbf{k} \times \mathbf{F} - \mathbf{k} \times \theta' \nabla_h \Pi, \quad (2)$$

where $\zeta = (\zeta_h, \zeta_z) + 2\mathbf{\Omega}$ is the absolute vorticity with $\mathbf{\Omega}$ being the rotation vector of the earth and where \mathbf{F} is the horizontal force per unit mass due to molecular effects and sub-grid-scale eddy momentum fluxes. The last term on the right in (2) is identically zero in pressure and isentropic coordinates and is small in geometric coordinates except in highly baroclinic situations. We will ignore this term in what follows.

Taking the vertical component of the curl of the momentum equation (1) results in the flux form of the vorticity equation:

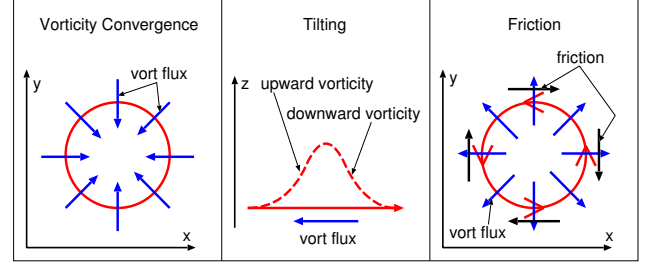
$$\frac{\partial \zeta_z}{\partial t} = -\nabla_h \cdot \mathbf{Z}. \quad (3)$$

This demonstrates that the Eulerian tendency of the vertical component of absolute vorticity equals the horizontal convergence of the horizontal flux of vertical vorticity. This result was emphasised by Haynes and McIntyre (1987).

The three panels of Fig. 1 illustrate the physical mechanisms behind the first three terms of the vorticity flux (2). The first term and panel represent simple bulk transport of vertical vorticity by the horizontal flow. Thus, if there is net mass convergence in the presence of positive absolute vorticity, as illustrated in the left panel of Fig. 1, there is also vorticity convergence and increasing vorticity with time.

The second term and panel illustrate a more subtle process. Upward motion in the presence of horizontal vortex

Fig. 1. Illustration of the physical effect of each of the first three terms in the vorticity flux. See text for further explanation.



lines lifts these lines. If the ascent covers a limited area, then the vortex lines are deformed as shown in the middle panel of Fig. 1. The initially horizontal vortex line (solid) exhibits zero vertical vorticity. However, with the ascending motion, the vortex line deforms into the dashed line, resulting in positive vertical vorticity on the left side of the middle panel and negative vertical vorticity on the right side. This corresponds to a flux of vertical vorticity from right to left. This mechanism is sometimes called 'tilting'. It results in the creation of a vorticity tendency dipole, with the positive and negative components located on opposite sides of the updraft with orientation normal to the vertical shear of the horizontal wind represented by the vortex lines.

The third term reflects the effect of the specific frictional force \mathbf{F} . The right panel of Fig. 1 shows the effect of a frictional force opposing a counterclockwise circulation. The result is a flux of vorticity away from the center of the circulation. The flux is directed normal to \mathbf{F} and to its left.

With minor manipulation, (2) and (3) along with the mass continuity equation

$$\frac{1}{\rho} \frac{d\rho}{dt} + \nabla \cdot \mathbf{v} = 0, \quad (4)$$

where ρ is the air density, yield the advective form of the vorticity equation:

$$\rho \frac{d(\zeta_z/\rho)}{dt} - \zeta_z \frac{\partial v_z}{\partial z} - \zeta_h \cdot \nabla_h v_z + \nabla_h \cdot (\mathbf{k} \times \mathbf{F}) = 0. \quad (5)$$

This equation is perfectly valid, but a misguided approximation that makes it look like an equation for a conserved scalar variable was made by a number of authors, e.g. Reed and Johnson (1974), Daggupaty and Sikka (1977), Shapiro (1978), Cho et al. (1979). The approximation omits the stretching and tilting terms (terms two and three in the above equation), from which the foregoing authors infer that vertical vorticity is transported conservatively from low to high levels. This inference leads one to conclude, for instance, that convection can act as a source of vertical vorticity in the upper troposphere by advecting vorticity-rich air from the lower troposphere to these levels. This is a conclusion that simple consideration of the Kelvin circulation theorem shows to be invalid in an area-averaged sense; the (absolute) circulation around a loop on a horizontal surface (technically, an isentropic surface, but the difference is

generally insignificant) does not change according to the Kelvin theorem. Thus, there is nothing a cumulus cloud totally confined within the loop can do to change that circulation, though it can change the local distribution of vorticity within the loop. The stretching and tilting terms work together with advection to enforce Kelvin’s theorem, and their omission disrupts this intricate dance, leading to erroneous conclusions. Transport of mass into the upper troposphere by convective updrafts can increase the area of a circulation loop surrounding the convective outflow at these levels, thereby decreasing the mean absolute vorticity within the loop, but this effect has nothing to do with the vertical transport of vertical vorticity.

In 1980 Richard Rotunno (personal communication) addressed the commonly made errors regarding the vertical transport of vertical vorticity in a manuscript that unfortunately was never published. The papers by Esbensen et al. (1987) and Haynes and McIntyre (1987) finally exposed these errors in the peer reviewed literature. We bring up this ‘ancient history’ because one occasionally sees the error reappearing in modern papers.

An Eulerian version of the circulation theorem may be derived from (3). Integrating over some fixed area A and applying the divergence theorem results in

$$\frac{d\Gamma}{dt} = - \oint_{\partial A} \mathbf{Z} \cdot \mathbf{n} dl. \quad (6)$$

The quantity

$$\Gamma = \int_A \zeta_z dA \quad (7)$$

is the absolute circulation around the periphery of A and the right side of (6) is the outward flux of vorticity through this periphery ∂A . Thus, the circulation around a system of interest responds to processes within the system only to the extent that they affect the vorticity flux on the boundary of the area defined by the circulation loop. In particular, dipole vorticity source-sink terms associated with vertical motion confined within the loop do not affect the circulation.

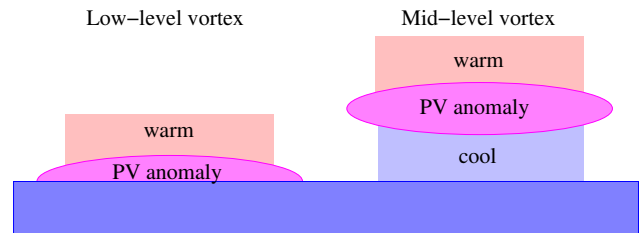
Often a system being analysed is moving with respect to the earth. It is generally desirable to analyse such a system in a co-moving reference frame. The vorticity flux can be transformed to this frame by making the substitution $\mathbf{v}_h \rightarrow \mathbf{V} + \mathbf{v}_h$ where \mathbf{V} is the horizontal velocity of the system and the new \mathbf{v}_h is the wind velocity relative to the moving system. The vorticity flux thus becomes

$$\mathbf{Z} \rightarrow \mathbf{V}\zeta_z + \mathbf{Z}. \quad (8)$$

(The vorticity is, of course, unchanged by this transformation, as \mathbf{V} is not a function of position.) The vorticity equation then transforms to

$$\frac{\partial \zeta_z}{\partial t} + \mathbf{V} \cdot \nabla_h \zeta_z = -\nabla_h \cdot \mathbf{Z}. \quad (9)$$

Fig. 2. Thermal response of the atmosphere to low- and mid-level vortices.



However, we recognise the left side of this equation as the Eulerian time rate of change of vorticity in the reference frame of the moving system, which is precisely the quantity that interests us. Thus, the final substitution

$$\frac{\partial ()}{\partial t} + \mathbf{V} \cdot \nabla () \rightarrow \frac{\partial ()}{\partial t} \quad (10)$$

reduces (9) to the original vorticity equation (3) which now applies in the moving frame. In other words, the original vorticity equation is invariant to Galilean transformations and is therefore unchanged when applied in a moving reference frame as long as the velocity and the vorticity tendency are interpreted as being relative to that frame. Similar considerations apply to the Eulerian circulation theorem (6).

Thermodynamic response to vorticity distribution

Vorticity distributions in the atmosphere are associated with corresponding balanced thermal perturbations. This can be understood from the point of view of the thermal wind, but the theory of potential vorticity inversion (Gent and McWilliams 1983, Hoskins et al. 1985, Thorpe 1985, Davis 1992, Raymond 1992, 1994) yields a more compact way of looking at this phenomenon.

Of particular interest is the response of the thermal structure to limited area potential vorticity anomalies at various levels in the atmosphere. The Ertel potential vorticity is defined

$$q = \frac{\zeta \cdot \nabla \theta}{\rho} \approx \frac{\zeta_z}{\rho_0} \frac{\partial \theta_0}{\partial z} \quad (11)$$

where θ is the potential temperature. The approximation on the right side of (11) is qualitatively valid for weak mesoscale vortices in mild shear, as the omitted term $(\zeta_h/\rho_0) \cdot \nabla_h \theta$ scales with the square of the shear in the balanced flow case. In this case the potential vorticity can be approximately inferred from the vertical component of absolute vorticity ζ_z , the ambient static stability $\partial \theta_0(z)/\partial z$, and the ambient density $\rho_0(z)$.

For the case of an isolated region of positive potential vorticity perturbation concentrated near a particular altitude, the air below the potential vorticity maximum tends to be

cooler than the environment at the same level away from the potential vorticity anomaly, and warmer above. This is illustrated in the right panel of Fig. 2. If the potential vorticity anomaly is located just above the surface, one sees just the warm anomaly, as indicated in the left panel of this figure.

Temperature anomalies in developing tropical cyclones are typically of order 1 K and have a ‘penetration depth’ D that defines their vertical extension from the centre of the potential vorticity anomaly given roughly by

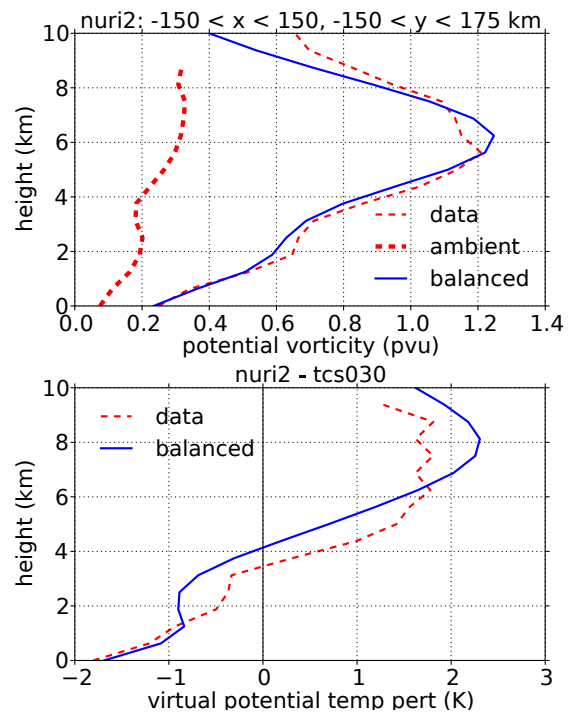
$$D = (f/N)R \quad (12)$$

where f is the Coriolis parameter, N is the Brunt-Väisälä frequency, and R is the horizontal radius of the potential vorticity anomaly. If $f/N \approx 5 \times 10^{-3}$ and $R \approx 300$ km, then $D \approx 1.5$ km. If the actual potential vorticity anomaly has vertical extent greater than D (as it generally does), the problem is close enough to being linear that the superposition principle can be used. So, if the potential vorticity anomaly extends from, say, 1–9 km, with a maximum near 5 km, one can expect a deep cold anomaly below a transition level typically somewhat less than the level of maximum potential vorticity and a corresponding warm anomaly above the transition level.

Though weak by tropical storm standards, potential vorticity anomalies in tropical waves and depressions are still strong enough to require the use of nonlinear balance rather than geostrophic balance. The resulting inversion equations are sufficiently nonlinear to require special inversion techniques, as outlined by Davis (1992) and Raymond (1992). Figure 3 shows an example from Raymond (2012) of a potential vorticity inversion for the case of a strong tropical depression on the verge of developing into typhoon *Nuri* (2008) (see Montgomery et al. 2010, Raymond and López 2011, Raymond et al. 2011, Montgomery and Smith 2012). The potential vorticity distribution in this case is idealised, as described by Raymond (2012). The main point is that the potential temperature perturbation predicted by the potential vorticity inversion is not far from the observed perturbation pattern, indicating that the thermodynamics and dynamics are in approximate balance in this case. Similar results are found for other cases. Davis and Trier (2007) arrived at comparable conclusions for mesoscale convective vortices over land.

The importance of the above result is that the balanced potential temperature profile in a region with vorticity structure typical of a tropical depression provides a thermodynamic environment for convection that is altered from that which occurs in the undisturbed tropics. As we now see, this modification of the environment causes significant alterations in the structure and strength of convection.

Fig. 3. Horizontally averaged potential vorticity (upper panel) and virtual potential temperature perturbation relative to undisturbed tropical conditions (lower panel) for a developing tropical cyclone. The thick dashed red line in the upper panel represents the ambient potential vorticity, while the thinner dashed red lines represent areally averaged observations in both panels. The solid blue lines show the averages over a corresponding region in the balanced model result. One potential vorticity unit (pvu) is $10^{-6} \text{ K m}^2 \text{ kg}^{-1} \text{ s}^{-1}$. Taken from Raymond (2012).



The effect of convection on spin up

The vertical circulations associated with deep, moist convection are crucial to tropical cyclogenesis via their effects on the vorticity budget. Convection in turn is influenced by the dynamic and thermodynamic environment provided by the incipient cyclone. Both aspects of the problem are considered here, with an attempt to highlight what we do not know as well as what we know.

At some point in the development of a tropical cyclone, the highly rotational nature of the cyclogenetic environment will affect the characteristics of the convection. The point in genesis where this becomes important is still uncertain; it would seem to be a question of the relative time scales of rotation and convective evolution. Hendricks et al. (2004) and Montgomery et al. (2006) in their ‘vortical hot tower’ hypothesis suggest that rotation may affect aspects of convection such as lateral entrainment quite early in cyclone formation. However, Wissmeier and Smith (2011) showed that the effects of rotation on entrainment and maximum updraft and downdraft velocities were small for their modelled clouds growing in environments with an effective Coriolis parameter ten times the tropical ambient, a value

typical of tropical depressions.

Convectively induced circulations can affect the first three terms of the horizontal vorticity flux. As Bretherton and Smolarkiewicz (1989) and Mapes (1993) showed, the environment responds to the imposition of a heat source and the resulting vertical motion by rapidly establishing consistent horizontal inflows and outflows extending to large distances from the heat source. These flows develop outward at the speed of gravity waves with the vertical scale of the flow pattern. Thus, after a short period, the first term in the vorticity flux convergence, $-\nabla_h \cdot (\mathbf{v}_h \zeta_z)$, establishes itself over a large area, at least for the smaller vertical wavenumber components of the originating vertical mass flux profile.

The second term, $\nabla_h \cdot (\zeta_h v_z)$, generally has a much more localised effect, corresponding to the fact that convective updrafts and downdrafts tend to be small in scale. The resulting vorticity tendency dipoles tend to cancel out in averaging operations such as the computation of a circulation tendency of a tropical disturbance. However, weak systematic transport of vorticity toward or away from the inner core can occur in the presence of system-scale vertical shear of the azimuthal wind. In particular, system circulation increasing with height in conjunction with net ascent transports vorticity away from the centre, while circulation decreasing with height in the presence of ascent does the reverse.

The third term, $-\nabla_h \cdot (\mathbf{k} \times \mathbf{F})$, is generally thought to act only in the boundary layer, and we will treat it this way in the current paper. However, to the extent that the vertical eddy transport of horizontal momentum within cumulus convection is important, this term could be active throughout the troposphere. More work needs to be done on this subject.

Due to the widespread vorticity convergence and divergence induced by vertical mass fluxes, the factors governing such fluxes in convection are of critical interest to tropical cyclogenesis. (Vertical mass fluxes outside of convection in tropical regions are largely the result of gravity waves and are therefore transient. They are thus likely to be inconsequential for the dynamics of cyclogenesis.)

Environmental control of convection

The concept of gross moist stability (GMS), first introduced by Neelin and Held (1987), is useful for quantifying the role of vertical mass fluxes in the thermodynamic interactions of convection with the environment. In Neelin and Held's (1987) model, the GMS Δm is the increase needed in the moist static energy m of a parcel in the lower troposphere for it to rise to the upper troposphere in moist convective updrafts. This increase in m is supplied by the net moist static energy source due to surface fluxes and radiative losses of moist static energy at the top of the troposphere. The smaller Δm is, the stronger is the convective mass flux per unit area. Raymond et al. (2009) provide a general discussion of gross moist stability.

Raymond et al. (2007) and Raymond and Fuchs (2009) defined a modified form of Neelin and Held's GMS, calling it the normalised gross moist stability (NGMS). The NGMS differs from the GMS in the following aspects: (1) It is defined for a continuous vertical coordinate rather than a two layer model; (2) the specific moist entropy is used in place of the moist static energy as the quasi-conserved variable; (3) the vertically integrated moisture convergence is used in place of the integrated mass divergence in the lower layer; and (4) horizontal advective flow through the control volume is included in the NGMS and excluded from the GMS.

Figure 4 shows a sketch of the lateral currents of entropy and water vapor in and out of a control volume ($E_{IN}, R_{IN}, E_{OUT}, R_{OUT}$) as well as the upward currents of these quantities at the surface (E_S, R_S) and at the tropopause ($E_T; R_T$ is assumed to be zero). The loss of water substance to precipitation is given by the precipitation current P . Currents of entropy and water substance contained completely within the control volume are important for the internal redistribution of entropy and water vapour, but do not enter directly into the control volume budget. For a control volume of unit horizontal area, these quantities become fluxes, i.e., currents per unit area.

The NGMS is defined in terms of the above currents as

$$\gamma = \frac{T_R(E_{OUT} - E_{IN})}{L(R_{IN} - R_{OUT})} \rightarrow \frac{T_R(E_S - E_T)}{L(P - R_S)} \quad (13)$$

where T_R is a constant reference temperature and L is the latent heat of condensation. The right-hand expression is the NGMS in the equilibrium case in which the lateral entropy divergence is in balance with the net source in the control volume from surface and tropopause entropy fluxes and in which the moisture convergence equals the precipitation minus surface evaporation rates. Irreversible entropy generation is ignored in this picture.

Figure 5 illustrates top-heavy and bottom-heavy vertical

Fig. 4. Sketch of quantities needed to define the normalised gross moist stability. See text for more information.

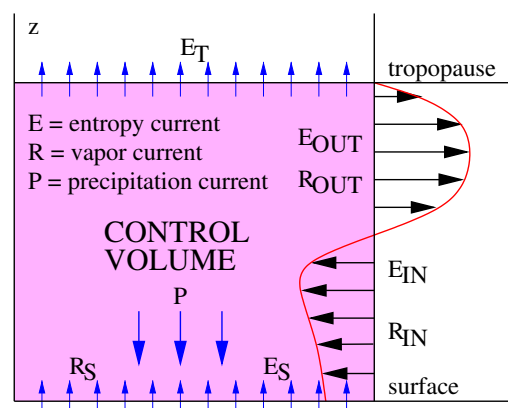
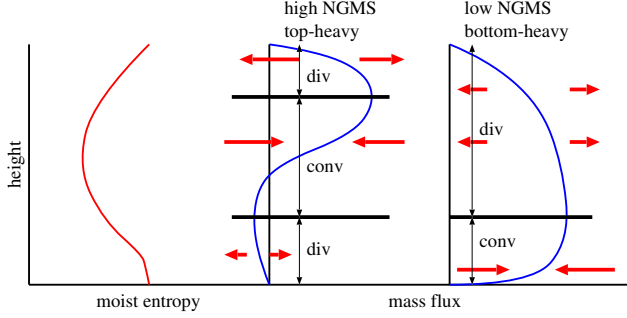


Fig. 5. Lateral mass flows in and out of a convective control volume (red arrows) for top-heavy and bottom-heavy vertical mass flux profiles (blue). The red curve on the left represents a typical moist entropy profile over warm oceans.



mass flux profiles and the effects of these profiles on the lateral entrainment and detrainment of entropy. Given a typical tropical profile of moist entropy (left panel), the top-heavy mass flux profile has most of its lateral inflow concentrated at middle levels where the value of the specific entropy is smaller than at levels above and below. Most of the outflow is at upper levels with some at lower levels where the moist entropy is larger. The net lateral export of entropy ($E_{OUT} - E_{IN}$) is thus much larger than it is for a bottom-heavy mass flux profile, where the primary inflow is at low levels where specific entropy values are large compared to middle levels. The NGMS is therefore smaller for bottom-heavy than for top-heavy profiles.

The existence of small and possibly negative values of the vertical mass flux in the lower troposphere is generally thought to be the result of a near-balance between updraft and mesoscale downdraft mass fluxes there. The mesoscale downdrafts occur when convection is dominated by large, organised convective systems with widespread stratiform rain areas. Bottom-heavy profiles occur when these systems do not exist (Zipser, 1969, 1977; Houze, 1977; Leary and Houze, 1980; López and Raymond, 2005; etc.).

The equilibrium precipitation rate can be predicted if the surface and tropopause fluxes of entropy and water vapour and the NGMS are known. Solving (13) for P , we find

$$P = R_S + \frac{T_R(E_S - E_T)}{L\gamma}, \quad (14)$$

which shows that for a given entropy forcing $E_S - E_T$ and surface evaporation rate R_S , the equilibrium precipitation rate increases as the NGMS decreases. In a result reminiscent of Neelin and Held (1987), the rate increases without bound as the NGMS $\gamma \rightarrow 0$. The task is then to relate the value of the NGMS to the properties of the environment in which the convection is embedded.

Moisture quasi-equilibrium

The equilibrium state of the atmosphere that occurs in (13) when $E_{OUT} - E_{IN} \rightarrow E_S - E_T$ and $R_{IN} - R_{OUT} \rightarrow P - R_S$ is generally considered to be stable in the sense that if the net rainfall rate differs from the net moisture convergence or the lateral entropy export differs from the surface minus tropopause entropy flux, convective and other processes tend to push these quantities back into balance. Simple theoretical calculations (Raymond, 2000) also suggest that the timescale for return to equilibrium becomes much shorter as the equilibrium moisture convergence and rainfall rate increase.

Sobel et al. (2007) and Sessions et al. (2010) present calculations suggesting that an unstable equilibrium may exist under certain conditions, with slight perturbations in rainfall rate pushing the system away from this equilibrium point. (See also Raymond et al., 2009.) In this case, two stable equilibrium points appear to exist, a moist state with rainfall rate greater than that of the unstable equilibrium point and a dry state with very small or zero rainfall rate.

The stability of an equilibrium precipitation state may be analysed using the vertically integrated budgets of moist static energy and water vapour. Using the analysis of Raymond et al. (2007), but in the current notation, the specific moist entropy s and water vapor mixing ratio r budgets become

$$\frac{d\bar{s}}{dt} + E_{OUT} - E_{IN} = E_S - E_T \quad (15)$$

and

$$\frac{d\bar{r}}{dt} + R_{OUT} - R_{IN} = R_S - P \quad (16)$$

where

$$\overline{(\quad)} = \frac{1}{g} \int (\quad) dp \quad (17)$$

with the pressure integral being from the tropopause to the surface. The irreversible generation of entropy is ignored in (15).

In the tropics the temperature profile does not change much, which means that variations in moist entropy are mostly due to variations in water vapour mixing ratio, which means that

$$\frac{d\bar{s}}{dt} \approx \frac{L}{T_R} \frac{d\bar{r}}{dt}. \quad (18)$$

Using the definition of NGMS (13) to eliminate $R_{OUT} - R_{IN}$ and $E_{OUT} - E_{IN}$ between (15) and (16) results in a tendency equation for the precipitable water \bar{r} :

$$(1 + \gamma) \frac{d\bar{r}}{dt} = \gamma (R_S - P) + \frac{T_R}{L} (E_S - E_T). \quad (19)$$

Setting $d\bar{r}/dt = 0$ reduces (19) to the equilibrium precipitation rate equation (14).

Imagine a situation in which the precipitation rate P is a monotonically increasing function of the precipitable water \bar{r} . If \bar{r} and P are perturbed positively from their equilibrium states without anything else changing, then (19) predicts that the precipitable water will acquire a negative tendency, thus forcing both the precipitable water and the precipitation rate back toward their equilibrium states, as long as the $\gamma > 0$. If on the other hand $\gamma < 0$, then the precipitable water and precipitation rate will increase without bound, or at least until non-linearity becomes important. Negative perturbations of \bar{r} and P will result in similar excursions in the negative direction.

It is clear from the above analysis (subject to the monotonicity requirement) that positive NGMS results in a stable equilibrium for P and \bar{r} while negative NGMS results in instability. This result justifies the use of the word ‘stability’ in the term gross moist stability.

Thermodynamic characterisation of tropical environments

Two parameters appear to be sufficient to characterise a large fraction of the observed variability in tropical convective environments and in NGMS in particular. The saturation fraction, defined as the ratio of precipitable water to saturated precipitable water is

$$S = \bar{r}/r^* \tag{20}$$

where r^* is the saturation mixing ratio. This concept was introduced by Bretherton et al. (2004) as the column relative humidity. Bretherton et al. (2004) found that the satellite-derived mean precipitation rate over tropical oceans is a function of the saturation fraction, with precipitation increasing strongly from near zero above about $S = 0.7$. Raymond et al. (2007) found similar results over the more limited area of the eastern tropical Pacific and the southwest Caribbean (see Fig. 6). Note that $d\bar{r}/dt$ may be written \bar{r}^*dS/dt if temperature variations are small enough to result in negligible variations in \bar{r}^* .

Raymond et al. (2011) and Gjorgjievska et al. (2013) introduced the instability index parameter

$$\mathcal{I} = s_{low}^* - s_{mid}^* \tag{21}$$

where s_{low}^* and s_{mid}^* are the saturated moist entropy averaged over [1, 3] km and [5, 7] km respectively. The instability index is zero for moist-neutral environments and $\mathcal{I} > 0$ indicates moist convective (not conditional) instability between the two layers.

Figure 7 shows mean moist entropy and saturated moist entropy soundings for two pre-typhoon disturbances observed in T-PARC/TCS08 (see later section), one of which (Nuri2) intensified rapidly into a typhoon, the other

Fig. 6 Infrared brightness temperature and airborne radar rainfall rate vs. saturation fraction in the eastern tropical Pacific and southwest Caribbean. Taken from Raymond et al. (2007).

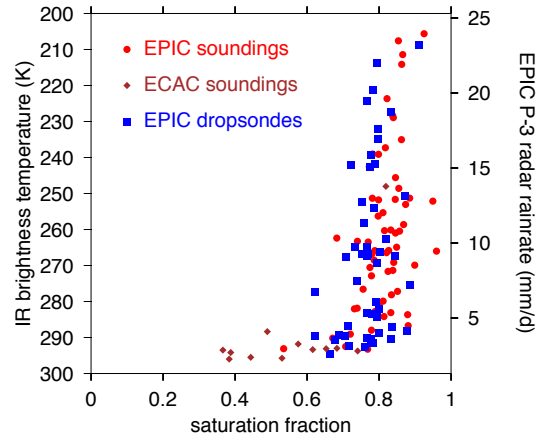
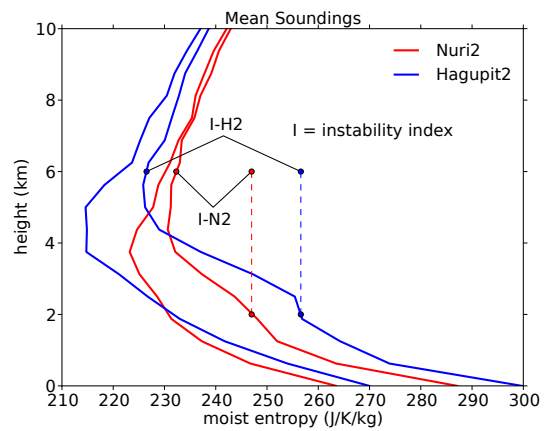


Fig. 7 Vertical profiles of moist entropy (left curves) and saturated moist entropy (right curves) averaged over two pre-typhoon disturbances observed in T-PARC/TCS08. Hagupit2 (blue) did not intensify for almost a week, whereas Nuri2 (red) became a tropical storm within 24 hr of the observation. The instability index, as defined by (21) was much larger for Hagupit2.



of which (Hagupit2) only intensified after a delay of about one week. As Fig. 7 shows, the instability index is much larger for Hagupit2 than for Nuri2. The correlation between small instability index and rapid intensification is somewhat counter-intuitive, but is not an accident, as we shall see below.

Figure 8 shows the difference between averaged virtual temperature profiles for Nuri2 and Hagupit2 implied by the entropy soundings in Fig. 7. Note that the difference in the upper and lower troposphere is of order 1 K and that virtual temperature effects are minor. These temperature differences likely reflect the balanced response to the different vorticity profiles in the Nuri2 and Hagupit2 cases. In particular, the strong mid-level vortex associated with Nuri2 is thought to produce the warm anomaly aloft and the cool anomaly at low levels absent in the Hagupit2 case. These anomalies

Fig. 8: Difference between mean Nuri2 and Hagupit2 temperature (blue) and virtual temperature (red) profiles.

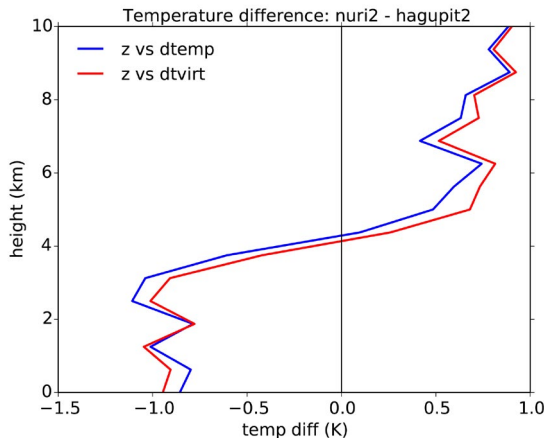
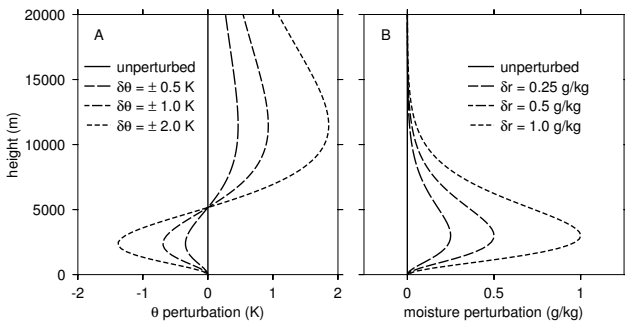


Fig. 9. Potential temperature and mixing ratio perturbations applied to the RCE reference profiles in WTG calculations. Taken from Raymond and Sessions (2007).



dominate the difference between the virtual temperature profiles for the two systems.

Cloud resolving model simulations

Certain types of calculations with cloud-resolving models yield insight into the behaviour of convection in varying thermodynamic environments. Raymond and Sessions (2007) showed in a cloud resolving model that profiles of virtual temperature and mixing ratio characteristic of convectively active regions of the tropics such as strong easterly waves and tropical depressions result in patterns of vertical mass flux that differ significantly from those that occur in less disturbed conditions. The model calculations were done in weak temperature gradient (WTG) mode in two dimensions. In WTG mode, a horizontal-mean vertical velocity called the WTG vertical velocity is assumed to produce horizontally uniform adiabatic cooling over the domain. This vertical velocity is adjusted so that the adiabatic cooling just counters the convective and radiative heating, forcing the horizontally averaged virtual potential temperature profile to equal a reference profile, assumed to be characteristic of the

immediate convective environment (Sobel and Bretherton, 2000; Raymond and Zeng, 2005; Raymond, 2007). In our version of WTG, the moisture undergoes vertical advection by the WTG vertical velocity and it is also entrained from a reference moisture profile in layers where the WTG vertical mass flux (WTG vertical velocity times density) increases with height.

In order to obtain initial reference profiles characteristic of the undisturbed tropics, the cloud resolving model is run to radiative-convective equilibrium (RCE) with an imposed surface wind speed of 5 m s^{-1} added to self-induced flows and with fixed sea surface temperature (SST). RCE is a reasonable approximation to mean, undisturbed tropical conditions, since the latitudinal export of energy out of the tropics is small compared to the vertical radiative and convective flows of energy (Peixoto and Oort, 1992). The potential temperature and mixing ratio profiles from this RCE computation are used as reference profiles for the initial WTG computations in which the imposed surface wind is varied over the range $[0, 20] \text{ m s}^{-1}$. Varying this wind is a convenient way of generating a range of surface heat and moisture fluxes. Subsequent WTG computations are made in which the reference profiles are modified by small amounts.

Figure 9 shows the vertical structure of the applied perturbations. The perturbations in potential temperature $\delta\theta$ are designed to mimic those produced by a mid-level potential vorticity anomaly, as illustrated in Figs 2 and 3, whereas those in mixing ratio δr increasingly moisten the lower troposphere.

Figure 10 shows the WTG vertical mass flux profiles in response to different values of $\delta\theta$ and δr , with an imposed wind speed of 7 m s^{-1} . As the right panel of Fig. 10 shows, the magnitude of the vertical mass flux increases as the reference profile moisture increases at fixed imposed wind speed and SST. However, the shape of the profile does not change much. In contrast, when $\delta\theta$ increases, the mass flux profile not only increases in magnitude but it also changes from top-heavy, with a maximum value near 8–10 km, to bottom-heavy, with a maximum near 5 km.

Given the dipolar vertical structure in the above potential temperature perturbations, larger values of $\delta\theta$ generally correspond to smaller values of the instability index \mathcal{I} . Similarly, larger δr corresponds roughly to larger values of the saturation fraction \mathcal{S} . As we shall see, these conditions also correspond to smaller NGMS. The theory of NGMS further implies higher precipitation rates in both cases. Fig. 11 verifies that the cloud resolving model supports these results.

Fig. 10. WTG vertical mass fluxes for an imposed surface wind of 7 m s^{-1} and the specified values of $\delta\theta$ (left panel) and δr (right panel). In the left panel $\delta r = 0$ and in the right panel $\delta\theta = 0$. Taken from Raymond and Sessions (2007).

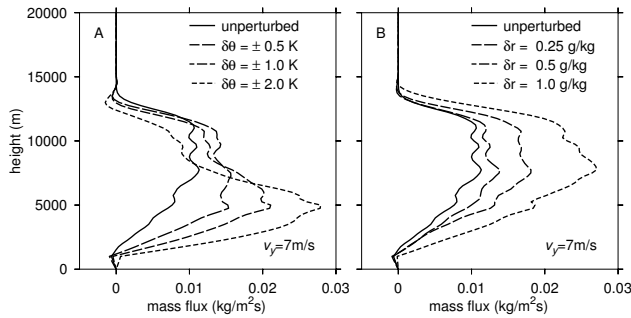
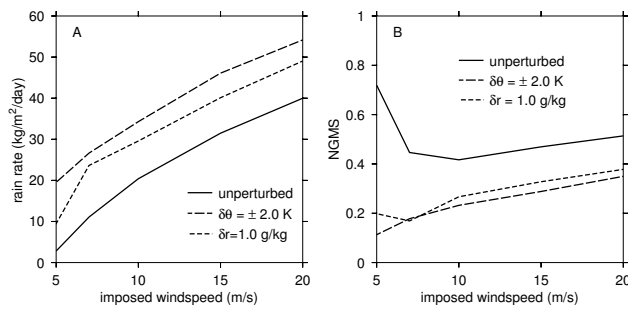


Fig. 11. Rainfall rate and NGMS as a function of imposed wind speed for different values of $\delta\theta$ and δr . Taken from Raymond and Sessions (2007).



Results from T-PARC/TCS08 and PREDICT

We first examine two pre-typhoon disturbances in detail and then generalise to the statistics of a wide range of potential tropical cyclogenesis events. The three cases are extracted from the T-PARC/TCS08 project and represent the first and second missions into pre-*Nuri* and the second mission into pre-*Hagupit*, designated *Nuri1*, *Nuri2*, and *Hagupit2*.

Figure 12 shows vertical profiles of circulation, circulation tendency, and vertical mass flux for the *Nuri2* case, based on results from Raymond et al. (2011). The mass flux profile is bottom-heavy, implying strong low-level convergence as a result of mass continuity, which is instrumental in the strong vorticity convergence associated with the large positive circulation tendency at low levels. The convergence-related spin-up tendency far exceeds the frictional spin-down tendency in this case. The tilting tendency is zero at the surface and somewhat negative below 4 km. The overall circulation tendency is positive up to 10 km, but largest at the surface. These strongly positive values are consistent with the subsequently observed rapid intensification of *Nuri*. The vertical profile of circulation at the time of measurement has a distinct maximum near 5 km.

Figure 13 presents the corresponding analysis for *Hagupit2*. As noted above, this weak wave was not intensifying at the time of observation and typhoon formation was delayed by nearly a week.

In contrast to *Nuri2*, *Hagupit2* exhibited a strongly top-heavy mass flux profile. There was actually mass and vorticity divergence up to about 2 km, resulting in net spin down of the circulation in this layer. However, the strong mid-level convergence centered near 5 km elevation resulted in a significant positive circulation tendency at middle levels. The circulation profile at the time of observation had a maximum at the surface, as is typical of west Pacific tropical waves (Reed and Recker, 1971).

Table 1 summarises calculations of saturation fraction, instability index, and NGMS for *Nuri1*, *Nuri2*, and *Hagupit2*. *Nuri2*, which was intensifying rapidly, had high saturation fraction, smaller instability index, and NGMS close to zero.

The small value of NGMS is particularly significant from the point of view of intensification, since in the steady state, only small entropy forcing is needed to produce very intense convection with strong precipitation and low-level mass (and hence vorticity) convergence, leading to rapid spin up.

Fig. 12. Vertical profiles for the precursor to typhoon *Nuri* on 16 August 2008 when it was a strong tropical depression. Left panel: Vertical profiles of planetary (red) and absolute (blue) circulation. Centre panel: Profiles of various circulation tendency terms as defined by (2) and (6). Right panel: Vertical profile of vertical mass flux. Plots based on data from Raymond et al. (2011).

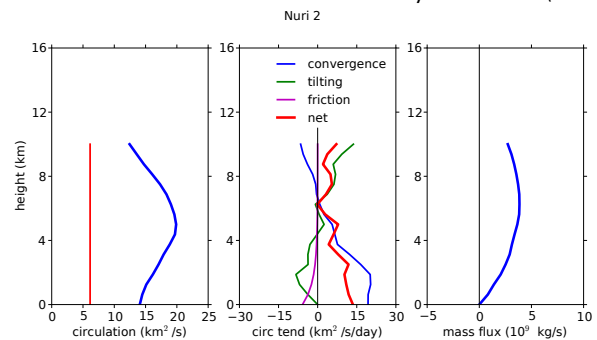


Fig. 13. As in Fig. 12 except for the precursor to typhoon *Hagupit* on 14 September 2008.

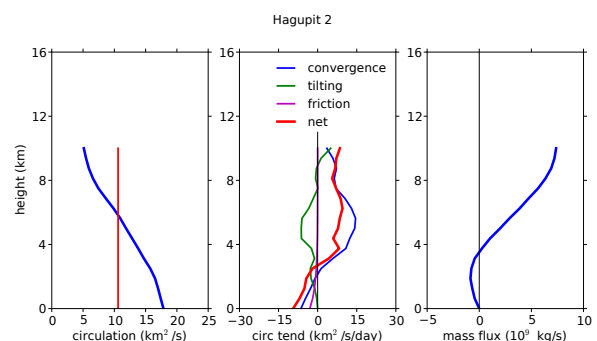


Table 1. Measured values of saturation fraction (S), instability index (I ; units $\text{J K}^{-1} \text{kg}^{-1}$), and normalised gross moist stability (NGMS) for the Nuri1, Nuri2, and Hagupit2 cases.

Case	Development	S	I	NGMS
Nuri1	intensifying	0.81	17	0.37
Nuri2	intensifying	0.88	11	-0.01
Hagupit2	notintensifying	0.82	27	0.64

In contrast, the saturation fraction is somewhat smaller for Hagupit2, the instability index is larger, and the NGMS is much larger, leading to much less precipitation and low-level mass convergence. This is consistent with the non-development of Hagupit in the time frame of the observations.

In accord with the numerical results of Raymond and Sessions (2007), the bottom-heavy vertical mass flux profile of Nuri2 is associated with a mid-level vortex of considerable strength. Furthermore, the lack of a mid-level vortex in the case of Hagupit2 is associated with top-heavy convection. A mid-level vortex can form via the action of top-heavy convection itself. As seen in the Hagupit2 case, top-heavy convection implies mid-level convergence, which results in vortex spin up at middle levels. Hagupit was apparently just beginning to form a mid-level vortex at the time of observation. Why this process took so long (about a week) for Hagupit is unknown, as we do not have observations over this period. In contrast, the mid-level vortex in Nuri2 formed in the 24-hour period between Nuri1 and Nuri2. As Fig. 14 shows, the maximum vorticity in Nuri1 was much weaker than in Nuri2 and was located much closer to the surface. Like Hagupit2, Nuri1 also exhibited top-heavy convection, which provides a plausible mechanism for the formation of the mid-level vortex in Nuri2. Nuri1 was otherwise distinguished from Hagupit2 by lower values of the instability index and the NGMS (see Table 1), suggesting that it was more prone to development.

To summarise, these results suggest that the formation of a mid-level vortex via the action of top-heavy convection, forced by some disturbance such as a tropical wave, followed by a new generation of convection with a bottom-heavy mass flux profile, is a viable pathway to the formation of a tropical cyclone. Many studies cited in the introduction support this idea, as do the numerical simulations of cyclogenesis by Bister and Emanuel (1997) and Nolan (2007).

The above results come from only two case studies, so it is important to see whether our conclusions are supported when more cases are considered. This is now addressed using 27 cases from the T-PARC/TCS08 and PREDICT experiments.

The upper left panel of Fig. 15 shows a scatter plot of the saturation fraction vs. the instability index for tropical disturbances studied in T-PARC/TCS08 and PREDICT (Gjorgjievska et al., 2013). The two variables are strongly anti-correlated, with moist environments being more stable. This is likely an expression of moisture quasi-

Fig. 14. As in Figure 12 except for the precursor to typhoon Nuri on 15 September 2008 (24 hr previous to Nuri2).

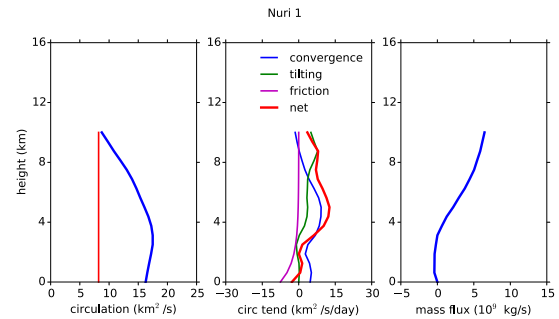
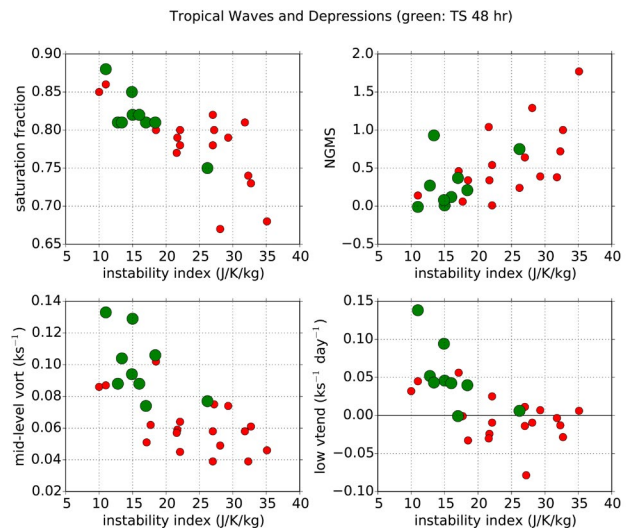


Fig. 15. Average saturation fraction vs. average instability index (upper left panel), normalised gross moist stability vs. instability index (upper right panel), mid-level mean absolute vorticity vs. instability index (lower left panel), and low-level mean vorticity tendency vs. instability index (lower right panel) for tropical disturbances observed by field programmes in the west Pacific (T-PARC/TCS08) and the Atlantic and Caribbean (PREDICT). The cases represented by large green dots intensified into tropical storms within 48 hr of the observations. The scaling on the NGMS eliminates two outlier cases in that plot only with large positive and negative values of the NGMS. Data from the analysis of Gjorgjievska et al. (2013) are used.



equilibrium as discussed above. Moist, stable disturbances were more likely to develop into tropical storms within 48 hours, as Fig. 15 indicates.

The upper right panel shows the NGMS vs. the instability index for the same sample, indicating that NGMS is correlated with instability index, such that disturbances with the lowest instability index (and the highest humidity) had the lowest NGMS. Systems with low NGMS are more likely to intensify rapidly in our sample.

The lower left panel shows that cases with a strong mid-level vortex, as indicated by large values of the mean vorticity in the [3, 5] km layer, are associated with small values of the

instability index. This is a manifestation of the balanced thermodynamic effects of a mid-level vortex. (By defining a vertical range for the maximum vorticity, we do not mean to imply that the vortex is totally confined within this range.)

Finally, the lower right panel of Fig. 15 shows that the instantaneous low-level vorticity tendency (averaged over the [0, 1] km layer) is strongly correlated with both low instability index and the tendency to form a tropical storm within 48 hours of the observation time.

Thus, Fig. 15 documents a consistent pattern in which a strong mid-level vortex interacts with convection to produce a balanced thermodynamic environment which is more stable and more moist than undisturbed tropical conditions. This environment favors further convection that is efficient in terms of precipitation production and effective in producing low-level spin up and tropical cyclogenesis due to its bottom-heavy mass flux profile. Stability and moisture are correlated, suggesting the existence of a moisture quasi-equilibrium principle in which convection drives the saturation fraction or column relative humidity toward an equilibrium value that increases as the instability index decreases.

Discussion and conclusions

As noted in the introduction, tropical cyclogenesis can occur in a broad variety of initial disturbances, such as various forms of tropical waves, monsoon troughs and gyres, and equatorward excursions of upper-level mid-latitude weather systems. However, many of these cases, particularly those occurring in the tropics, exhibit a common pathway to development in which a mid-level vortex precedes the spin up of an underlying low-level vortex.

It is hard to imagine that the mid-level vortex is incidental in this path to tropical cyclogenesis as suggested by Dunkerton et al. (2009), though we find many proposed explanations of this process to be vague or otherwise lacking. In particular, the flux form of the vorticity equation (3) shows conclusively that the vertical component of absolute vorticity is not transported vertically. This invalidates arguments that vorticity from the mid-level vortex is somehow carried downward in a way that increases the low-level circulation around the system of interest. The near-surface circulation can increase by only one mechanism: the convergence of the horizontal flux of vertical vorticity, of which the bulk inward transport of vorticity by the horizontal flow dominates. This competes with the tendency of surface friction to decrease the circulation there.

In the tropics, where isentropic surfaces tend to be flat and quasi-geostrophic upglide is minimal, this mass and moisture convergence is most likely related to the existence of convection of a form that, in the mean, lifts significant amounts of mass out of the boundary layer. If convective or mesoscale downdrafts bring a substantial flux of mass into the boundary layer, the net upward transport of mass out of the boundary layer can be significantly reduced or reversed.

The spin up of the low-level vortex thus depends on

the nature of the convection occurring within the vortex. Normal deep convection over the high SSTs of the western tropical Pacific and surrounding areas tends to exhibit top-heavy convective mass flux profiles due to the prevalence of large stratiform rain areas associated with the convection (Mapes and Houze, 1993, 1995; Back and Bretherton, 2006; López and Raymond, 2005; Raymond and López, 2011; Raymond et al., 2011). Similar results are found in the western Atlantic and Caribbean (Gjorgjievska and Raymond, 2013). Such convection has maximum lateral inflow in the mid-troposphere, with the result that aggregations of such convection result in the production of mid-level vortices. As these vortices develop, the mesoscale environment in the area covered by the vortex acquires a cool anomaly in the lower troposphere below the vortex and a warm anomaly in the upper troposphere. The convection occurring in this environment typically exhibits a much more bottom-heavy mass flux profile. This convection draws in air at low levels, resulting in mass and vorticity convergence there. The vorticity convergence can lead to the formation of the low-level vortex that signals tropical cyclogenesis.

The changes in virtual temperature in the upper and lower troposphere in the initial phase of spin up are of order 1 K. These values are small, but according to the cloud-resolving model simulations of Raymond and Sessions (2007), they are sufficient to produce a radical change in the vertical mass flux profile of modeled convection, reducing the level of maximum vertical mass flux from 9–10 km to 5 km. The difference in the observed mass flux profiles between Hagupit2 and Nuri2 (see Figs 12 and 13), in conjunction with the observed difference in the virtual temperature profile (Fig. 8), is consistent with the results of Raymond and Sessions (2007).

The instability index is a good measure of the small changes in the temperature profile produced by a mid-level vortex. As expected from considerations of balance, the instability index is inversely correlated with the strength of the mid-level vortex for a large sample of cases (lower left panel, Fig. 15). The instability index is also inversely correlated with the circulation tendency at low levels (lower right panel, Fig. 15) and a larger circulation tendency at low levels is an indication of tropical storm formation within 48 hr of the observation.

Evidence from our tropical cyclogenesis case studies indicates that the saturation fraction of the air in the vortex increases as the instability index decreases (see the upper left panel of Fig. 15). We take this as evidence for the existence of a 'moisture quasi-equilibrium' governed by the convection occurring in the vortex; if the saturation fraction is less than demanded by this quasi-equilibrium principle, convection contrives to increase it. If it is greater than the equilibrium value, the reverse occurs. Raymond (2000) explains this process using column-integrated moisture and entropy budgets plus the concept of gross moist stability. One of the results of this analysis is that the relaxation rate increases greatly as the convection becomes more active.

López and Raymond (2005) provide further evidence that moisture quasi-equilibrium acts in the tropical environment. These results, based on observations of convection in the western tropical Pacific, show that convection exports moist entropy laterally if the saturation deficit is small and imports entropy if it is large. (Larger saturation deficit implies smaller saturation fraction.) Since temperature profiles do not change much in space or time in the deep tropics, import of entropy tends to increase the saturation fraction while export has the reverse effect. Thus, the humidity of the environment appears to be regulated by the action of convection, which acts to drive the water vapour toward an equilibrium value in this case. Interestingly, convection with a bottom-heavy mass flux profile imports entropy while convection with a top-heavy profile exports it. This is in accord with the mechanics of gross moist stability as reviewed by Raymond et al. (2009).

Our present results provide further evidence that the equilibrium saturation fraction increases as the instability index decreases. If this analysis is correct, then convection by itself cannot increase the humidity in a region indefinitely (i.e., to 100 per cent), but only up to the equilibrium value for the environment in which it is embedded. In tropical cyclogenesis, it appears that the decrease in instability index (i.e. the stabilization of the environment) is the factor responsible for increasing the equilibrium saturation fraction. The increase in saturation fraction and the decrease in instability index both favour an increase in the average precipitation rate, while the decrease in instability index also favors more bottom-heavy mass fluxes. Both factors encourage stronger low-level mass and vorticity convergence, and hence tropical cyclogenesis. Furthermore, both are related to the formation of a strong, mid-level vortex.

We believe that the web of results reported in this review presents a compelling case for the importance of the mid-level vortex to tropical cyclogenesis. We also consider these results to be complementary to the idea of Dunkerton et al. (2009) of a protected pouch in a precursor disturbance. The ingestion of dry air into the forming tropical storm has the potential to disrupt all of the thermodynamic processes we have discussed. However, the importance of the mid-level vortex does suggest that the pouch should be defined to include it. This raises a problem in the early stages of tropical cyclogenesis in which the low-level and mid-level circulations can be displaced from each other by hundreds of kilometers. How the pouch should be defined reduces to the question as to whether the low-level or the mid-level circulation plays the more important dynamical role. In particular, what mechanisms bring the two into vertical alignment, those associated with the low-level or the mid-level circulations? Do the thermodynamics of a long-lasting mid-level circulation regenerate a low-level circulation directly under it or does the existing low-level circulation regenerate a new mid-level circulation directly above it? Or is there some alternative process that somehow causes the displaced vortices at the two levels to come into alignment?

These are among the questions that remain to be answered by future research.

As it stands, the theory of tropical cyclogenesis expressed in this paper does not take into account the possibility of upper-level influence, as discussed in the introduction. However, if upper level dynamical processes influence the virtual temperature profiles in middle and upper levels, then the properties of deep convection would be affected, possibly in a manner that influences tropical cyclogenesis. Though upper level dynamics has been invoked for many decades as a possible influence on tropical cyclogenesis, current theory is lacking in this area and remains to be developed.

There is some modeling evidence that tropical cyclogenesis can sometimes occur without the formation of a mid-level vortex previous to low-level spinup (e.g., Davis and Bosart, 2006; Nolan 2007). However observational confirmation of these results and more complete modeling diagnostics are needed to verify this possibility.

The present theory of cyclogenesis also needs to be extended to periods both before and after that covered here. We currently have little to say about how the initial formation of a mid-level vortex actually occurs, aside from the assertion that undisturbed tropical environments are conducive to convection with a top-heavy mass flux profile that is associated with mid-level convergence. More study is needed of disturbances that carry out this initial phase of tropical cyclogenesis. Similarly, at some point in the evolution of a developing cyclone, the vorticity becomes so large that the character of convection occurring in this environment must change. Where exactly this transition occurs remains to be determined.

Finally, the role of convective momentum transfer in tropical cyclones, particularly in their formation phase, needs to be assessed. The ELDORA Doppler radar data obtained during T-PARC/TCS08 should be of help in this task.

We believe that Bruce Morton would have been enchanted by the subtle interplay between vorticity and convection that occurs in tropical cyclogenesis.

Acknowledgments

We thank Michael Herman, Roger Smith, and an anonymous reviewer for useful comments. This work was supported by National Science Foundation Grant 1021049.

References

- Back, L. E. and Bretherton, C. S. 2006. Geographic variability in the export of moist static energy and vertical motion profiles in the tropical Pacific. *Geophys. Res. Letters*, 33, L17810, doi:10.1029/2006GL026672.
- Bister, M. and Emanuel, K. A. 1997. The genesis of hurricane *Guillermo*: TEXMEX analyses and a modeling study. *Mon. Wea. Rev.*, 125, 2662–82.
- Bosart, L. F. and Bartlo, J. 1991. Tropical storm formation in a baroclinic environment. *Mon. Wea. Rev.*, 119, 1979–2013.
- Bretherton, C. S., Peters, M. E., and Back, L. E. 2004. Relationships between water vapor path and precipitation over the tropical oceans. *J. Climate*, 17, 1517–28.
- Bretherton, C. S. and Smolarkiewicz, P. K. 1989. Gravity waves, compensating subsidence and detrainment around cumulus clouds. *J. Atmos. Sci.*, 46, 740–59.
- Challa, M., Pfeffer, R. L., Zhao, Q., and Chang, S. W. 1998. Can eddy fluxes serve as a catalyst for hurricane and typhoon formation? *J. Atmos. Sci.*, 55, 2201–19.
- Challa, M. and Pfeffer, R. L. 1980. Effects of eddy fluxes of angular momentum on model hurricane development. *J. Atmos. Sci.*, 37, 1603–18.
- Cho, H.-R., Cheng, L., and Bloxam, R. M. 1979. The representation of cumulus cloud effects in the large-scale vorticity equation. *J. Atmos. Sci.*, 36, 127–39.
- Davis, C. A. 1992. Piecewise potential vorticity inversion. *J. Atmos. Sci.*, 49, 1397–11.
- Davis, C. A. and Bosart, L. 2001. Numerical simulations of the genesis of hurricane *Diana* (1984). Part I: Control simulation. *Mon. Wea. Rev.*, 129, 1859–81.
- Davis, C. A. and Bosart, L. 2002. Numerical simulations of the genesis of hurricane *Diana* (1984). Part II: Sensitivity of track and intensity prediction. *Mon. Wea. Rev.*, 130, 1100–24.
- Davis, C. A. and Bosart, L. F. 2006. The formation of hurricane *Humberto* (2001): The importance of extra-tropical precursors. *Quart. J. Roy. Meteor. Soc.*, 132, 2055–85.
- Davis, C. A. and Trier, S. B. 2007. Mesoscale convective vortices observed during BAMEX. Part I: Kinematic and thermodynamic structure. *Mon. Wea. Rev.*, 135, 2029–49.
- Dickinson, M. and Molinari, J. 2000. Climatology of sign reversals of the meridional potential vorticity gradient over Africa and Australia. *Mon. Wea. Rev.*, 128, 3890–3900.
- Dickinson, M. J. and Molinari, J. 2002. Mixed Rossby-gravity waves and western Pacific tropical cyclogenesis. Part I: Synoptic evolution. *J. Atmos. Sci.*, 59, 2183–96.
- Dunkerton, T. J., Montgomery, M. T., and Wang, Z. 2009. Tropical cyclogenesis in a tropical wave critical layer: Easterly waves. *Atmos. Chem. Phys.*, 9, 5587–46.
- Dunn, G. E. 1940. Cyclogenesis in the tropical Atlantic. *Bull. Am. Meteor. Soc.*, 21, 215–29.
- Esbensen, S. K., Shapiro, L. J., and Tollerud, E. I. 1987. The consistent parameterization of the effects of cumulus clouds on the large-scale momentum and vorticity fields. *Mon. Wea. Rev.*, 115, 664–69.
- Ferreira, R. N. and Schubert, W. H. 1997. Barotropic aspects of ITCZ breakdown. *J. Atmos. Sci.*, 54, 261–85.
- Gent, P. R. and McWilliams, J. C. 1983. Consistent balanced models in bounded and periodic domains. *Dyn. Atmos. Oceans*, 7, 67–93.
- Gjorgjievska, S. and Raymond, D. J. 2014. Interaction between dynamics and thermodynamics during tropical cyclogenesis. *Atmos. Chem. Phys.*, 14, 3065–82.
- Gray, W. M. 1968. Global view of the origin of tropical disturbances and storms. *Mon. Wea. Rev.*, 96, 669–700.
- Harr, P. A., Kalafsky, M. S., and Elsberry, R. L. 1996a. Environmental conditions prior to formation of a midlevel tropical cyclone during TCM-93. *Mon. Wea. Rev.*, 124, 1693–1710.
- Harr, P. A., Elsberry, R. L., and Chan, J. C. L. 1996b. Transformation of a large monsoon depression to a tropical storm during TCM-93. *Mon. Wea. Rev.*, 124, 2625–43.
- Hartmann, D. L. and Maloney, E. D. 2001. The Madden-Julian oscillation, barotropic dynamics, and north Pacific tropical cyclone formation. Part II: Stochastic barotropic modeling. *J. Atmos. Sci.*, 58, 2559–70.
- Haynes, P. H. and McIntyre, M. E. 1987. On the evolution of vorticity and potential vorticity in the presence of diabatic heating and frictional or other forces. *J. Atmos. Sci.*, 44, 828–41.
- Hendricks, E. A., Montgomery, M. T., and Davis, C. A. 2004. The role of ‘vortical’ hot towers in the formation of tropical cyclone *Diana* (1984). *J. Atmos. Sci.*, 61, 1209–32.
- Hoskins, B. J., McIntyre, M. E., and Robertson, A. W. 1985. On the use and significance of isentropic potential vorticity maps. *Quart. J. Roy. Meteor. Soc.*, 111, 877–946.
- Houze, R. A. 1977. Structure and dynamics of a tropical squall-line system. *Mon. Wea. Rev.*, 105, 1540–67.
- Houze, R. A. Jr and coauthors. 2006. The hurricane rainband and intensity change experiment. *Bull. Am. Meteor. Soc.*, 1503–21.
- Leary, C. A. and Houze, R. A. 1980. The contribution of mesoscale motions to the mass and heat fluxes of an intense tropical convective system. *J. Atmos. Sci.*, 37, 784–96.
- López Carrillo, C. and Raymond, D. J. 2005. Moisture tendency equations in a tropical atmosphere. *J. Atmos. Sci.*, 62, 1601–13.
- Maloney, E. D. and Hartmann, D. L. 2001. The Madden-Julian oscillation, barotropic dynamics, and north Pacific tropical cyclone formation. Part I: Observations. *J. Atmos. Sci.*, 58, 2545–58.
- Mapes, B. E. 1993. Gregarious tropical convection. *J. Atmos. Sci.*, 50, 2026–37.
- Mapes, B. and Houze, R. A. jr 1993. An integrated view of the 1987 Australian monsoon and its mesoscale convective systems. II: Vertical structure. *Quart. J. Roy. Meteor. Soc.*, 119, 733–54.
- Mapes, B. and Houze, R. A. jr 1995. Diabatic divergence profiles in western Pacific mesoscale convective systems. *J. Atmos. Sci.*, 52, 1807–28.
- Molinari, J., Skubis, S., and Vollaro, D. 1995. External influences on hurricane intensity: Part III. Potential vorticity structure. *J. Atmos. Sci.*, 52, 3593–3606.
- Molinari, J., Knight, D., Dickinson, M., Vollaro, D., and Skubis, S. 1997. Potential vorticity, easterly waves, and eastern Pacific tropical cyclogenesis. *Mon. Wea. Rev.*, 125, 2699–2708.
- Montgomery, M. T., Nicholls, M. E., Cram, T. A., and Saunders, A. B. 2006. A vortical hot tower route to tropical cyclogenesis. *J. Atmos. Sci.*, 63, 355–86.
- Montgomery, M. T., Lussier, L. L. III, Moore, R. W., and Wang, Z. 2010. The genesis of Typhoon *Nuri* as observed during the Tropical Cyclone Structure 2008 (TCS-08) field experiment—Part 1: The role of the easterly wave critical layer. *Atmos. Chem. Phys.*, 10, 9879–9900.
- Montgomery, M. T. and coauthors. 2012. The pre-depression investigation of cloud systems in the tropics (PREDICT) experiment. *Bull. Am. Meteor. Soc.*, 93, 153–72.
- Montgomery, M. T. and Farrell, B. F. 1993. Tropical cyclone formation. *J. Atmos. Sci.*, 50, 285–310.
- Montgomery, M. T. and Smith, R. K. 2012. The genesis of typhoon *Nuri* as observed during the Tropical Cyclone Structure 2008 (TCS08) field experiment—Part 2: Observations of the convective environment. *Atmos. Chem. Phys.*, 12, 4001–09.
- Neelin, J. D. and Held, I. M. 1987. Modeling tropical convergence based on the moist static energy budget. *Mon. Wea. Rev.*, 115, 3–12.
- Nolan, D. S. 2007. What is the trigger for tropical cyclogenesis? *Aust. Met. Mag.*, 56, 241–66.
- Palmer, C. 1952. Tropical meteorology. *Quart. J. Roy. Meteor. Soc.*, 78, 126–64.
- Peixoto, J. P. and Oort, A. H. 1992. *Physics of climate*. American Institute of Physics, 520 pp.
- Pfeffer, R. L. 1956. A discussion of the balance of angular momentum in hurricanes. *Bull. Am. Meteor. Soc.*, 37, 234.
- Pfeffer, R. L. 1958. Concerning the mechanics of hurricanes. *J. Meteor.*, 15, 113–20.
- Pfeffer, R. L. and Challa, M. 1981. A numerical study of the role of eddy fluxes of momentum in the development of Atlantic hurricanes. *J. Atmos. Sci.*, 38, 2393–98.
- Raymond, D. J. 1992. Nonlinear balance and potential-vorticity thinking at large Rossby number. *Quart. J. Roy. Meteor. Soc.*, 118, 987–1015.
- Raymond, D. J. 1994. Nonlinear balance on an equatorial beta plane. *Quart. J. Roy. Meteor. Soc.*, 120, 215–19.
- Raymond, D. J. 2000. Thermodynamic control of tropical rainfall. *Quart. J. Roy. Meteor. Soc.*, 126, 889–98.

- Raymond, D. J. 2007. Testing a cumulus parametrization with a cumulus ensemble model in weak-temperature-gradient mode. *Quart. J. Roy. Meteor. Soc.*, *133*, 1073–85.
- Raymond, D. J., Sessions, S. L., and Fuchs, Ž. 2007. A theory for the spin-up of tropical depressions. *Quart. J. Roy. Meteor. Soc.*, *133*, 1743–54.
- Raymond, D. J. 2012. Balanced thermal structure of an intensifying tropical cyclone. *Tellus*, *64*, 19181, doi.org/10.3402/tellusa.v64i0.19181.
- Raymond, D. J. and Fuchs, Ž. 2009. Moisture modes and the Madden-Julian oscillation. *J. Climate*, *22*, 3031–46.
- Raymond, D. J., López-Carrillo, C., and López Cavazos, L. 1998. Case-studies of developing east Pacific easterly waves. *Q. J. R. Meteorol. Soc.*, *124*, 2005–34.
- Raymond, D. J. and López Carrillo, C. 2011. The vorticity budget of developing typhoon Nuri (2008). *Atmos. Chem. Phys.*, *11*, 147–63.
- Raymond, D. J. and Sessions, S. L. 2007. Evolution of convection during tropical cyclogenesis. *Geophys. Res. Letters*, *34*, L06811, doi:10.1029/2006GL028607.
- Raymond, D. J., Sessions, S. L., and Fuchs, Ž. 2007. A theory for the spin-up of tropical depressions. *Quart. J. Roy. Meteor. Soc.*, *133*, 1743–54.
- Raymond, D. J., Sessions, S. L., and López Carrillo, C. 2011. Thermodynamics of tropical cyclogenesis in the northwest Pacific. *J. Geophys. Res.*, *116*, D18101, doi:10.1029/2011JD015624.
- Raymond, D. J., Sessions, S., Sobel, A., and Fuchs, Ž. 2009. The mechanics of gross moist stability. *J. Adv. Model. Earth Syst.*, *1*, art. #9, 20 pp.
- Raymond, D. J. and Zeng, X. 2005. Modelling tropical atmospheric convection in the context of the weak temperature gradient approximation. *Quart. J. Roy. Meteor. Soc.*, *131*, 1301–20.
- Reed, R. J. and Johnson, R. H. 1974. The vorticity budget of synoptic-scale wave disturbances in the tropical western Pacific. *J. Atmos. Sci.*, *31*, 1784–90.
- Reed, R. J. and Recker, E. E. 1971. Structure and properties of synoptic-scale wave disturbances in the equatorial western Pacific. *J. Atmos. Sci.*, *28*, 1117–33.
- Riehl, H. 1948. On the formation of typhoons. *J. Meteor.*, *5*, 247–64.
- Ritchie, E. A. and Holland, G. J. 1993. On the interaction of tropical-cyclone-scale vortices II. discrete vortex patches. *Quart. J. Roy. Meteor. Soc.*, *119*, 1363–79.
- Ritchie, E. A. and Holland, G. J. 1997. Scale interactions during the formation of typhoon Irving. *Mon. Wea. Rev.*, *125*, 1377–96.
- Ritchie, E. A. and Holland, G. J. 1999. Large-scale patterns associated with tropical cyclogenesis in the western Pacific. *Mon. Wea. Rev.*, *127*, 2027–43.
- Rogers, R. F. and Fritsch, J. M. 2001. Surface cyclogenesis from convectively driven amplification of midlevel mesoscale convective vortices. *Mon. Wea. Rev.*, *129*, 605–37.
- Sadler, J. C. 1976. A role of the tropical upper tropospheric trough in early season typhoon development. *Mon. Wea. Rev.*, *104*, 1266–78.
- Sadler, J. C. 1978. Mid-season typhoon development and intensity changes and the tropical upper tropospheric trough. *Mon. Wea. Rev.*, *106*, 1137–52.
- Sessions, S. L., Sugaya, S., Raymond, D. J., and Sobel, A. H. 2010. Multiple equilibria in a cloud-resolving model using the weak temperature gradient approximation. *J. Geophys. Res.*, *115*, D12110, doi:10.1029/2009JD013376.
- Shapiro, L. J. 1978. The vorticity budget of a composite African tropical wave disturbance. *Mon. Wea. Rev.*, *106*, 806–17.
- Simpson, J., Ritchie, E., Holland, G. J., Halverson, J., and Stewart, S. 1997. Mesoscale interactions in tropical cyclone genesis. *Mon. Wea. Rev.*, *125*, 2643–61.
- Sobel, A. H., Bellon, G., and Bacmeister, J. 2007. Multiple equilibria in a single-column model of the tropical atmosphere. *Geophys. Res. Letters*, *34*, L22804, doi:10.1029/2007GL031320.
- Sobel, A. H. and Bretherton, C. S. 2000. Modeling tropical precipitation in a single column. *J. Climate*, *13*, 4378–92.
- Thorpe, A. J. 1985. Diagnosis of balanced vortex structure using potential vorticity. *J. Atmos. Sci.*, *42*, 397–406.
- Wang, C.-C. and Magnusdottir, G. 2005. ITCZ Breakdown in three-dimensional flows. *J. Atmos. Sci.*, *62*, 1497–1512.
- Wang, C.-C. and Magnusdottir, G. 2006. The ITCZ in the central and eastern Pacific on synoptic time scales. *Mon. Wea. Rev.*, *134*, 1405–21.
- Wang, Z., Montgomery, M. T., and Dunkerton, T. J. 2010a. Genesis of pre-hurricane Felix (2007). Part I: The role of the easterly wave critical layer. *J. Atmos. Sci.*, *67*, 1711–29.
- Wang, Z., Montgomery, M. T., and Dunkerton, T. J. 2010b. Genesis of pre-hurricane Felix (2007). Part II: Warm core formation, precipitation evolution, and predictability. *J. Atmos. Sci.*, *67*, 1730–44.
- Wissmeier, U. and Smith, R. K. 2011. Tropical cyclone convection: The effects of ambient vertical vorticity. *Quart. J. Roy. Meteor. Soc.*, *137*, 845–57.
- Zipser, E. J. 1969. The role of organized unsaturated convective downdrafts in the structure and rapid decay of an equatorial disturbance. *J. Appl. Meteor.*, *8*, 799–814.
- Zipser, E. J. 1977. Mesoscale and convective scale downdrafts as distinct components of squall-line structure. *Mon. Wea. Rev.*, *105*, 1568–89.

